

Appearance of enhanced tissue features in narrow-band endoscopic imaging

Kazuhiro Gono

Olympus Co.
Ishikawa-cho, Hachioji-shi
Tokyo 192-8507
Japan
and
Tokyo Institute of Technology
Imaging Sciences and Engineering Laboratory
4259 Nagatsuda-cho, Midoriku, Yokohama-shi,
Kanagawa 226-8503
Japan

Takashi Obi

Masahiro Yamaguchi

Tokyo Institute of Technology
Imaging Sciences and Engineering Laboratory
4259 Nagatsuda-cho, Midoriku, Yokohama-shi
Kanagawa 226-8503
Japan

Nagaaki Ohyama

Tokyo Institute of Technology
Frontier Collaborative Research Center
Kanagawa 226-8503
Japan

Hirohisa Machida

Yasushi Sano

Shigeaki Yoshida

National Cancer Center Hospital East
Department of Gastroenterology and Endoscopy
6-5-1 Kashiwanoha, Kashiwa-shi
Chiba 277-8577
Japan

Yasuo Hamamoto

Takao Endo

Sapporo Medical University
First, Department of Internal Medicine
S-1, W-16, Chuo-ku
Sapporo 060-8543
Japan

1 Introduction

A video endoscope system is now considered an indispensable tool for the diagnosis of early-stage gastrointestinal disease. In recent years, endoscopic therapy has attracted a great deal of interest because of the advantages of minimally invasive techniques. To improve the chances for total tumor resection by endoscopic means, early detection is mandatory. To detect these early cancers, it is important to precisely observe the color variation and fine structural pattern of the mucosa. Kudo et al.^{1–3} reported that estimating the pathology of a colon polyp is possible by observing the crypt orifice (the so-called pit pattern) of colonic glands with a magnified endoscope. Tobita⁴ reported the usefulness of the classification of minute

Abstract. This study was performed to examine the usefulness of medical endoscopic imaging utilizing narrow-band illumination. The contrast between the vascular pattern and the adjacent mucosa of the underside of the human tongue was measured using five narrow-band illuminations and three broadband illuminations. The results demonstrate that the pathological features of a vascular pattern are dependent on the center wavelength and the bandwidth of illumination. By utilizing narrow-band illumination of 415 ± 30 nm, the contrast of the capillary pattern in the superficial layer was markedly improved. This is an important benefit that is difficult to obtain with ordinary broadband illumination. The appearances of capillary patterns on color images were evaluated for three sets of filters. The narrow, band imaging (NBI) filter set (415 ± 30 nm, 445 ± 30 nm, 500 ± 30 nm) was selected to achieve the preferred appearance of the vascular patterns for clinical tests. The results of clinical tests in colonoscopy and esophagoscopy indicated that NBI will be useful as a supporting method for observation of the endoscopic findings of early cancer. © 2004 Society of Photo-Optical Instrumentation Engineers. [DOI: 10.1117/1.1695563]

Keywords: endoscopic imaging; narrow-band illumination.

Paper 03025 received Mar. 4, 2003; revised manuscript received Jun. 23, 2003 and Aug. 21, 2003; accepted for publication Aug. 22, 2003.

gastric mucosal patterns, which was proposed by Sakaki,⁵ for diagnosing the depressed type of early gastric cancers.

Chromoscopy has been used widely to precisely observe the fine structural patterns of the mucosa.^{6,7} Chromoscopy is a contrast staining method using a biocompatible dye agent, such as indigo carmine or methylene blue. In the mucosa with glands, the dye agents accumulate within crypt orifices. Although chromoscopy is effective in many applications, this method still has some problems, such as difficulty in achieving complete and even coating of the mucosal surface with the dye, the extra cost of the equipment for dye spraying, the dye agent itself, and the extra time required to perform the procedure. Kumagai et al.⁸ reported that observation of an intrapapillary capillary loop pattern is potentially useful for diagnosing the depth of invasion of early esophageal cancer. Several investigations have been conducted on the diagnosis of early

Address all correspondence to Kazuhiro, Gono. Olympus Co., Ishikawa-cho, Hachioji-shi, Tokyo 192-8507, Japan. Tel: 81-45-924-5183; E-mail: gono@isl.titech.ac.jp

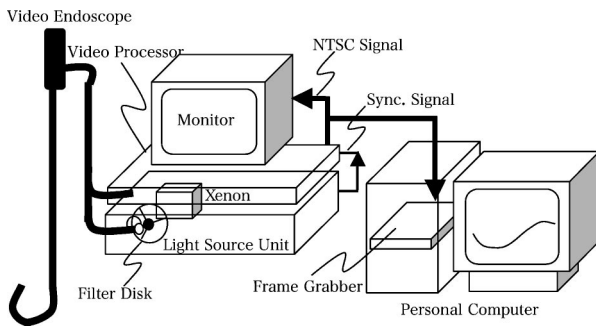


Fig. 1 Medical video endoscope system using the RGB sequential illumination method.

gastric cancer through observation of the capillary patterns on the gastric mucosa.⁹ However, chromoscopy is not useful for enhancing the imaging of the capillary patterns. To resolve the problems of chromoscopy, we proposed narrow-band imaging (NBI).¹⁰ This is a medical video endoscope system utilizing narrow-band illumination. Narrow-band illuminations are created with three optical interference filters in which the bandwidths are spectrally narrowed.

Sano et al.¹¹ conducted preliminary clinical tests of NBI during colonoscopy. They reported that imaging of the colonic mucosa with NBI provides enhanced pit pattern contrast compared with ordinary observation. However, a quantitative understanding of the relation between spectral features of the illumination and tissue features of the observational image is still lacking. Kienle et al.¹² investigated how the wavelength of the illumination affects the reproduced color of the vein under the skin using a tissue phantom. They used a thin glass tube phantom containing whole blood in a lipid colloid. It is, however, unclear how the contrast of the thinner vasculature, such as the capillaries, depends on the center wavelength of the filtered illumination.

2 Experiment

This study was performed to determine the basis for tissue imaging by narrow-band illumination and to confirm the clinical benefits of NBI. Three experiments were conducted as follows.

- Experiment 1: The contrasts between the vascular and the adjacent mucosa of the underside of the human tongue were evaluated quantitatively using five narrow-band illuminations and three broadband illuminations. We discuss how the center wavelength and the bandwidth of illumination affect the contrast of the vascular pattern.

- Experiment 2: Color images of the underside of the human tongue were observed using three sets of filters selected from five narrow-band filters and three broadband filters. The appearance of the capillary pattern was evaluated using CIE 1976 L*a*b* color difference and L* contrast.
- Experiment 3: Clinical tests were performed in colonoscopy and esophagoscopy (Barrett's esophagus) by comparing the standard system and NBI.

3 Materials and Methods

3.1 Medical Video Endoscope System

The medical video endoscope system shown in Fig. 1 was used in the present study. The light source unit (CLV-U40, Olympus Optical, Tokyo, Japan) has a xenon lamp and a filter disk. Three optical interference filters are mounted on the filter disk. Red, green, blue (R,G,B) filters are ordinarily used and divided visible wavelength ranges into three bands. The video endoscope has a light guide of an optical fiber bundle and a monochrome CCD at its tip. R,G,B illuminations irradiate the mucosa sequentially via the light guide as the filter disk rotates. The monochromatic image signal corresponding to each filtered illumination is formed by synchronizing the sequential illumination process and the conversion process by the CCD. Analog signals read from the CCD are transformed sequentially to digital signals in the video processor (CV240, Olympus Optical). To display a color image on a monitor (OEV-142, Olympus Optical), each monochromatic image signal (band image) is assigned to an R/G/B color channel. Then, the R/G/B color signals are sent out to the monitor as National Television System Committee (NTSC) television signals. These signals become input signals of the frame grabber (METOR II/MC4; Matrox Electronic Systems, Dorval, Canada). The frame grabber can digitize television signals with a sampling of 640×480 pixels. Moreover, the gray levels in each pixel are quantized with integer values from 0 to 255.

3.2 Experiment 1: Contrast Between the Vascular Pattern and the Adjacent Mucosa of the Tongue

The contrast between the vascular pattern and the adjacent mucosa of the underside of the human tongue was evaluated quantitatively. The structure of the vascular pattern of the human tongue is similar to that of the gastrointestinal mucosa,^{14,15} therefore, this tissue was appropriate for our study. Evaluations were performed using eight different illuminations. Five narrow-band filters and three broadband filters were used. The center wavelengths and bandwidths are listed in Table 1. F6, F7, and F8 have the same specifications as the filters utilized in the ordinary light source unit. F1, F4,

Table 1 Center wavelength and bandwidth of filters.

	F1	F2	F3	F4	F5	F6	F7	F8
Wavelength	415 nm	445 nm	500 nm	540 nm	600 nm	420 nm	540 nm	610 nm
Bandwidth	30 nm	30 nm	30 nm	20 nm	20 nm	100 nm	80 nm	80 nm

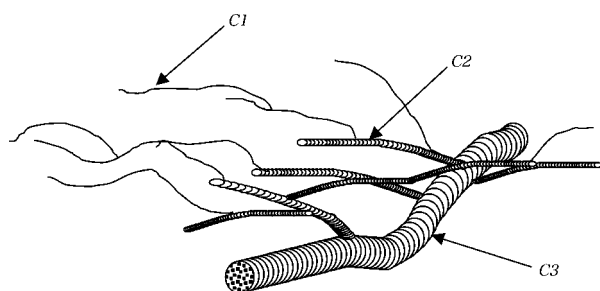


Fig. 2 Structure of the blood vessels in the human tongue. C1 indicates the fine capillaries in the superficial mucosa. C2 indicates the thick capillaries in regions deeper than C1. C3 indicates the thick veins in regions deeper than C1 and C2.

and F5 were selected to investigate the influence of bandwidth by comparison with F6, F7, and F8. Narrow-band filters F2 and F3 were selected for evaluation of the changes in contrast within a short wavelength range. In this range, the molar excitation coefficient of the hemoglobin changes most sharply in the visible range.¹³

A magnified video endoscope (GIF-Q240Z, Olympus) was used to observe the vascular pattern. This apparatus has an 80-fold optical magnifying capacity. Operating the knob at the handle grip allows switching between the wide view and the telescopic view. Experiments observing the human tongue were performed with the telescopic view to visualize the capillaries. In the telescopic view, because of the small depth of field of the optics, it is difficult to fix the focus. Measuring the contrast requires sharp focus. A transparent silicone cap was attached to the tip of the video endoscope. A stable sharp focus was obtained by placing the tip of the cap gently on the tissue. Although using the cap changes the blood flow slightly, we assumed that the change in blood flow has little effect on the contrast of the vascular pattern. Indeed, placing the cap gently on the mucosa was accompanied by little if any change in the vascular pattern. Fixing the gain of the video processor maintained the signal-to-noise ratio of images at a uniform level. The dark noise was automatically subtracted from the analog signal of the CCD. The images were stored in a personal computer as digital data. Before measuring the contrast, the tone of the image was transformed since its gamma equals unity.

Figure 2 shows the schema of the vascular patterns. A dense capillary bed is typically found in superficial layers of the mucosa, and thicker blood vessels run in deeper layers. The difference in blood vessel depth may influence the contrast of the image. Therefore, to examine the influence of the depth of blood vessels on contrast, we classified the vascular patterns into three types by thickness and depth in the mucosa. The capillaries found in the superficial mucosa were classified as class 1 (C1 pattern). The thicker vasculature in deeper layers was classified as class 2 (C2 pattern). Thick veins were classified as class 3 (C3 pattern). The thicknesses of C1, C2 and C3 patterns are about 10 to 20, 20 to 50, and 200 to 500 μm , respectively.

In this study, the contrast was defined as the luminance ratio according to Weber's law,¹⁶ as shown in Eq. (1). In this definition, a pixel value of 8 bits (0 to 255) was used to calculate substitution for the luminance.

Table 2 Filter sets and assignments of band image to color channel for color imaging.

	Blue	Green	Red
Set A	F1	F2	F3
Set B	F1	F4	F5
Set C	F6	F7	F8

$$ctr = |g_v - g_m| / g_m, \quad (1)$$

where g denotes the pixel value of the recorded image and subscripts v and m refer to the vascular pattern and its adjacent mucosa, respectively. The positions of blood vessels were selected manually by observation. After the position of the blood vessel was selected, the position of its adjacent mucosa was selected from an area where no blood vessel could be seen. Two hundred and fifty such selections were conducted for the three classes of vascular pattern. As a result, 250 contrast values were obtained in each filter for the class of vascular pattern. The differences in average contrast values among the different filters and the different classes of blood vessel were evaluated statistically. In our experiments, it could not be assumed that variances of the pair to be compared were equal. Therefore, the test statistic of Aspin-Welch [Eq. (2)] was employed¹⁷:

$$t_o = \frac{\bar{c}_1 - \bar{c}_2}{\sqrt{\frac{s_1^2}{n_1} + \frac{s_2^2}{n_2}}}, \quad (2)$$

where \bar{c}_1 and \bar{c}_2 denote averages calculated from 250 contrast values, s_1^2 and s_2^2 denote variances, and n_1 and n_2 denote number of samples ($n_1 = n_2 = 250$). This is distributed approximately as a Student's t distribution with the degree of freedom ν shown as Eq. (3).

$$\nu = \frac{\left(\frac{s_1^2}{n_1} + \frac{s_2^2}{n_2}\right)^2}{\frac{\left(\frac{s_1^2}{n_1}\right)^2}{n_1 - 1} + \frac{\left(\frac{s_2^2}{n_2}\right)^2}{n_2 - 1}}. \quad (3)$$

In this study, one-sided hypothesis tests were performed. The p value was deduced from the t distribution table as the probability $p = \Pr\{|t| \geq t_o\} / 2$. A p value of 1% or less ($p < 0.01$) was taken to indicate significance.

3.3 Experiment 2: Appearance of C1 Pattern on Color Images of the Tongue

Combinations of filters for color imaging are listed in Table 2. Set C included the same combination as that utilized in the ordinary light source unit. To evaluate the effects of narrowing bandwidth, Set B was selected as having center wavelengths similar to those of Set C. We selected filters for Set A by placing importance on the imaging of the capillaries. There are many variations in the relation between band image and

Table 3 xy chromaticity coordinates of a primary color in the color monitor.

	Red	Green	Blue
x	0.63	0.29	0.15
y	0.33	0.60	0.06

color channel. In this study, we simply assigned R/G/B color channels as a function of wavelength. Evaluations of the appearance of the C1 pattern were performed with these three sets of filters. Two criteria, CIE 1976 $L^*a^*b^*$ color difference and the contrast based on L^* , were used.

The CIE 1976 $L^*a^*b^*$ color difference¹⁸ is calculated by:

$$dE = \sqrt{(L_v^* - L_m^*)^2 + (a_v^* - a_m^*)^2 + (b_v^* - b_m^*)^2}, \quad (4)$$

where the subscripts v and m represent the $L^*a^*b^*$ values calculated from the pixel values sampled from the vascular patterns and the adjacent mucosa, respectively. CIE 1976 $L^*a^*b^*$ values were deduced from CIE XYZ tristimulus values by Eq. (5):

$$L^* = 116 \left(\frac{Y}{Y_w} \right)^{1/3} - 16, \quad a^* = 500 \left[\left(\frac{X}{X_w} \right)^{1/3} - \left(\frac{Y}{Y_w} \right)^{1/3} \right],$$

$$b^* = 200 \left[\left(\frac{X}{X_w} \right)^{1/3} - \left(\frac{Z}{Z_w} \right)^{1/3} \right], \quad (5)$$

where X_w , Y_w , and Z_w are XYZ tristimulus values of white. This white is the color displayed on the monitor with pixel values $(R,G,B) = (255,255,255)$. XYZ tristimulus values are deduced from RGB pixel values by Eq. (6):

$$\begin{bmatrix} X \\ Y \\ Z \end{bmatrix} = \begin{bmatrix} \frac{x_R}{y_R} & \frac{x_G}{y_G} & \frac{x_B}{y_B} \\ 1 & 1 & 1 \\ \frac{1-x_R-y_R}{y_R} & \frac{1-x_G-y_G}{y_G} & \frac{1-x_B-y_B}{y_B} \end{bmatrix} \times \begin{bmatrix} \frac{Y_{R \max}}{255} & 0 & 0 \\ 0 & \frac{Y_{G \max}}{255} & 0 \\ 0 & 0 & \frac{Y_{B \max}}{255} \end{bmatrix} \begin{bmatrix} R \\ G \\ B \end{bmatrix}, \quad (6)$$

where tones of R,G,B are linearized by the gamma correction curve of the video endoscope system. $Y_{R \max}$, $Y_{G \max}$, and $Y_{B \max}$ are luminance with the maximum pixel value ($= 255$) and x_i and y_i , ($i=R,G,B$) are xy chromaticity coordinates of the primary color displayed on the monitor calculated by Eq. (7):

$$x_i = \frac{X_i}{X_i + Y_i + Z_i}, \quad y_i = \frac{Y_i}{X_i + Y_i + Z_i}, \quad (i=R,G,B). \quad (7)$$

The xy chromaticity coordinates of a primary color are shown in Table 3. L^* contrast is calculated by Eq. (8) in the same way as in Eq. (1):

$$L^*ctr = |L_v^* - L_m^*| / L_m^*. \quad (8)$$

The positions of capillary and adjacent mucosa on the image were selected in the same way as described in experiment 1.

3.4 Experiment 3: Clinical Tests

3.4.1 Colonoscopy

Since most colorectal cancers are thought to develop from adenomatous polyps,¹⁹ early removal via polypectomy is ef-

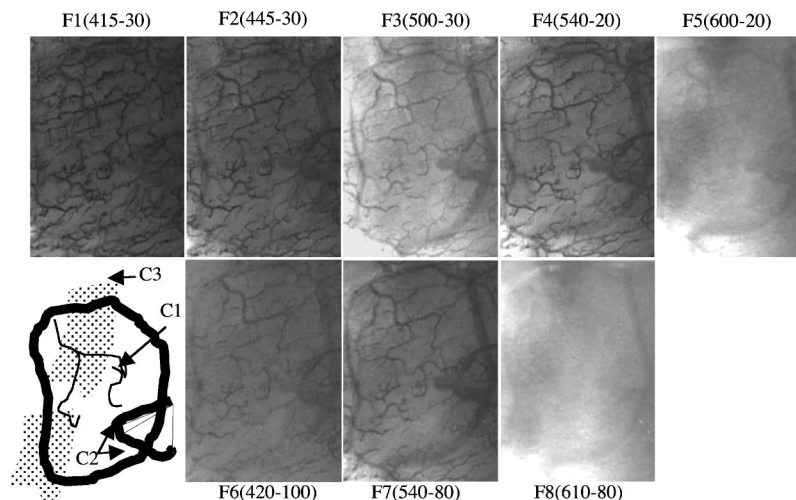


Fig. 3 Narrow-band images and broadband images of the underside of the human tongue. (Top) Narrow-band images (F1 to F5). (Bottom) Broadband images (F6 to F8). (Bottom left) Diagrammatic representation of the blood vessel classes.

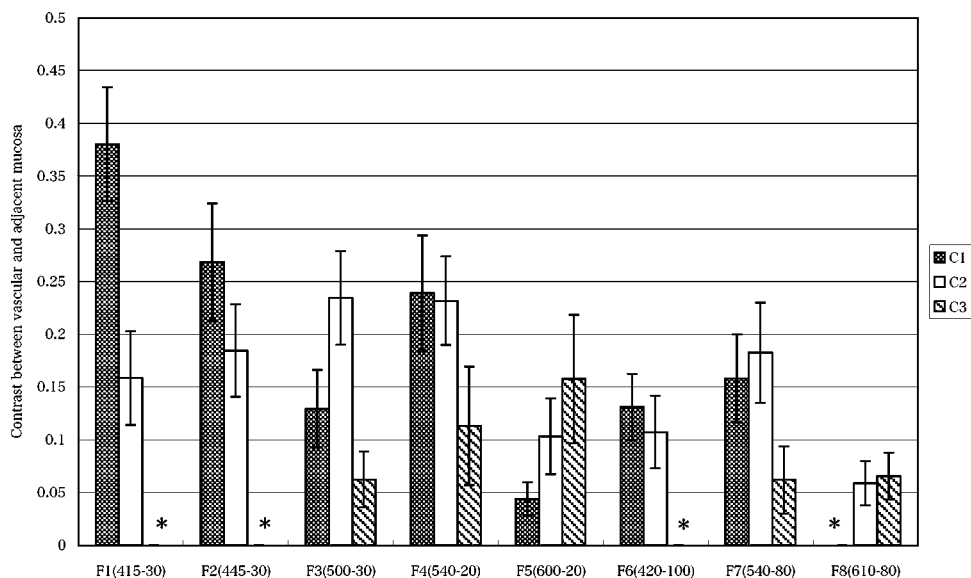


Fig. 4 Contrast between each class of blood vessels and the neighboring mucosa. The asterisks in the figure indicate that the contrast could not be calculated because the blood vessel could not be seen. The error bars indicate 1 standard deviation $n = 250$.

fective for reducing the incidence of colorectal cancer.²⁰ In colonoscopy, it is not easy to find small adenomatous polyps in the early stages. To confirm the effectiveness of NBI for visualizing small adenomatous polyps, clinical tests were performed at the National Cancer Center Hospital East in Chiba, Japan.

The apparatus for the clinical test was almost the same as that shown in Fig. 1. However, one more light source unit was added to allow comparison of NBI and the ordinary system. Switching between both light source units was performed by detaching and inserting the connector of the endoscope from or to the light source unit. The filter set that was used in the NBI examination process was set A for the reasons discussed in Sec. 5. Although a magnifying endoscope (PCF-Q240ZI, Olympus) was employed, evaluations were performed with the wide view endoscope. Twenty-seven patients gave their informed consent to participate in this study. The average diameter of small polyps was 5.6 mm. The pathologies of all specimens obtained by biopsy indicated that they were adenomatous. Endoscopic procedures were performed by a gastroenterologist experienced in the technique of colonoscopy. The patients first underwent standard colonoscopy using a conventional light source. Then NBI observation was performed with the endoscope still in place.

The visualization of small adenomatous polyps by both methods was evaluated. These images were scored by the en-

doscopists using a visual scale defined as follows: unseen (score 1), unclear (score 2), clear (score 3). The differences in visualization for both of the light sources were evaluated by a one-sided hypothesis test performed in the way same as in experiment 1.

3.4.2 Barrett's esophageal endoscopy

Barrett's esophagus (BE) is defined as the replacement of the normal squamous epithelium by a columnar-lined esophagus with specialized intestinal metaplasia (SIM). The incidence of esophageal adenocarcinoma in patients with BE is about 30- to 40-fold higher than that in the general population. The number of cases of esophageal adenocarcinoma is currently increasing at a rate faster than rates for breast, lung, and colon cancers in western countries.²¹ The poor prognosis for patients with Barrett's esophageal cancer is due both to the lack of an effective method for early detection, which would enable curative excision, and the inability to prevent metastatic disease. Endo et al.²² reported that diagnosis based on pit patterns in the BE mucosa using magnified chromoendoscopy is useful for detecting the SIM portion. To confirm the effectiveness of NBI for visualization of the pit pattern of BE, clinical tests were performed at Sapporo Medical University, Sapporo, Japan.

Table 4 p values of statistical analyses.

	F1	F2	F3	F4	F5
C1:F1	—	2.73×10^{-27}	4.52×10^{-110}	1.40×10^{-40}	9.71×10^{-139}
C2:F4	4.47×10^{-20}	8.49×10^{-20}	0.36	—	7.70×10^{-58}
C3:F5	*	*	9.21×10^{-26}	1.29×10^{-5}	—

* Contrast could not be calculated.

The filter set that was used in the NBI examination process was Set A. A magnifying video endoscope (GIF-Q240Z, Olympus) was employed. The configuration and the test procedure were the same as that described for colonoscopy. Twelve patients gave their informed consent to participate in this study. All of the patients had previously been diagnosed with BE and were being followed up in an endoscopic surveillance program at Sapporo Medical University Hospital. The endoscopic procedures were performed by a gastroenterologist experienced in the technique of magnification endoscopy for detection of BE. The patients first underwent standard endoscopy and then magnification endoscopy. The illumination unit for the conventional observation was then changed to NBI observation with the endoscope still in place, and magnifying endoscopy by NBI was performed immediately after exchange of the illumination unit.

Visualization of the pit patterns on the BE mucosa by the two methods was evaluated. These images were scored by the endoscopists using a visual scale defined as follows: completely impossible (score 1), visualization just possible (score 2), fairly sharp visualization (score 3), complete visualization possible (score 4). The differences in visualization between the two light sources were evaluated by a one-sided hypothesis test performed in the same way as in experiment 1.

4 Results

4.1 Experiment 1: Contrast Between the Vascular Pattern and the Adjacent Mucosa of the Tongue

The images produced by the five narrow-band filters and three broadband filters are shown in Fig. 3. The relationships between the vascular patterns and classification are also illustrated schematically in Fig. 3. Considering images F1 to F5, it is clear that the appearance of the vascular patterns depends on the class of the blood vessels and the center wavelength of the narrow-band filter. C1 patterns were seen in the F1 image. However, fine features, such as the tip of the capillary, were blurred in the F2 image. Furthermore, such fine features were difficult to see in the F4 image and could not be seen at all in the F5 image. In F3 and F4 images, although the C1 pattern was blurred, the C2 pattern could be seen more clearly than in the F1 image. In the F5 image, the C1 and C2 patterns were blurred. The C3 pattern was also blurred in the F5 image. However, the F5 image seemed to be appropriate for visualizing the C3 pattern. Examination of F1 and F6 indicated that narrowing the bandwidth improves visualization of the C1 pattern. The effects of narrowing bandwidth on visualization of the C2 and C3 patterns are unclear.

Figure 4 shows the average values of the contrast in each class and in each band image. The asterisks in the figure indicate that the contrast could not be calculated because the vascular patterns could not be determined manually. The error bars represent 1 standard deviation. The average values were in good agreement with the results of the observations described earlier. The p values are listed in Table 4.

The results for the C1 patterns demonstrated a statistically significant difference in a comparison of F1 images, which have a higher contrast than the other band images ($p < 0.01$). The results for the C2 pattern indicated no statistically significant differences between F4 and F3 images ($p = 0.36$). The results also demonstrated a statistically significant

difference with F4 images, which have a higher contrast than the other band images ($p < 0.01$). The results for C3 patterns demonstrated a statistically significant difference in F5 images, which have a higher contrast of C3 vasculature than the other band images ($p < 0.01$). For the C1 pattern, F1 images showed significantly higher contrast for blood vessels than F6 images ($p = 8.52 \times 10^{-11}$). For the C2 pattern, F4 images had a higher contrast for blood vessels than F7 images, and this difference was statistically significant ($p = 9.30 \times 10^{-10}$). For the C3 pattern, F5 images showed a significantly higher contrast for blood vessels than F8 images ($p = 1.63 \times 10^{-97}$).

4.2 Experiment 2: Appearance of C1 Pattern in Colored Images of the Tongue

Figure 5 shows colored images of the underside mucosa of the human tongue. The color in Figs. 5(b) and 5(c) is a natural reddish tissue color. On the other hand, that shown in Fig. 5(a) is different from the others. However, the C1 pattern could be seen more clearly in Fig. 5(a). The upper row in Table 5 shows the results of CIE 1976 $L^*a^*b^*$ color difference (dE) between the C1 pattern and the adjacent mucosa. The value of dE in Set B was significantly larger than both that of Set A ($p = 2.77 \times 10^{-21}$) and that of Set C ($p = 6.18 \times 10^{-32}$). The lower row in Table 5 shows the results of L^*ctr . The value of L^*ctr in Set A was significantly larger than those of Set B ($p = 2.28 \times 10^{-28}$) and Set C ($p = 1.83 \times 10^{-25}$).

The results from CIE 1976 $L^*a^*b^*$ color differences indicated that Set B is an appropriate filter set for color imaging. On the other hand, the results from L^*ctr indicated that Set A is an appropriate filter set for color imaging. The color images shown in Fig. 5 indicate that L^*ctr is more suitable than CIE 1976 $L^*a^*b^*$ color differences for evaluating the appearance of the blood vessels. This is discussed in detail in Sec. 5.

4.3 Experiment 3: Clinical Tests

4.3.1 Colonoscopy

As an example of a clinical test, images obtained in a case of familial adenomatosis coli are shown in Fig. 6. In the NBI image, the typical branching pattern of blood vessels can be seen as a blue pattern. Moreover, small polyps of familial adenomatosis coli can be seen more clearly than those in the conventional image. The small polyps in NBI images can be seen as brown staining. The pathology of most small polyps are adenomatous, and such polyps show angiogenesis in the superficial layer of the mucosa, which can be detected in the F1 and F2 images. As a result, most of the small polyps can be seen clearly as brown staining. Table 6 shows the results from scoring by a gastroenterologist using a visual scale. The

Table 5 CIE 1976 $L^*a^*b^*$ color difference and contrast of L^* of C1 pattern.

	Set A	Set B	Set C
dE	13.96 ± 3.98	18.19 ± 5.47	12.17 ± 5.24
L^*ctr	0.19 ± 0.07	0.12 ± 0.06	0.12 ± 0.06

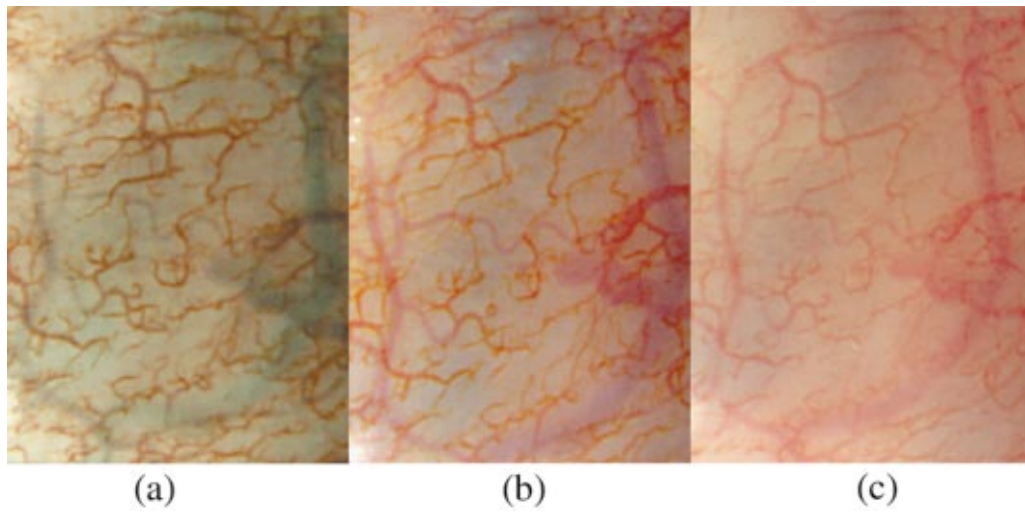


Fig. 5 Color images of the underside of the human tongue. (a) Filter Set A. (b) Filter Set B. (c) Conventional broadband filters.

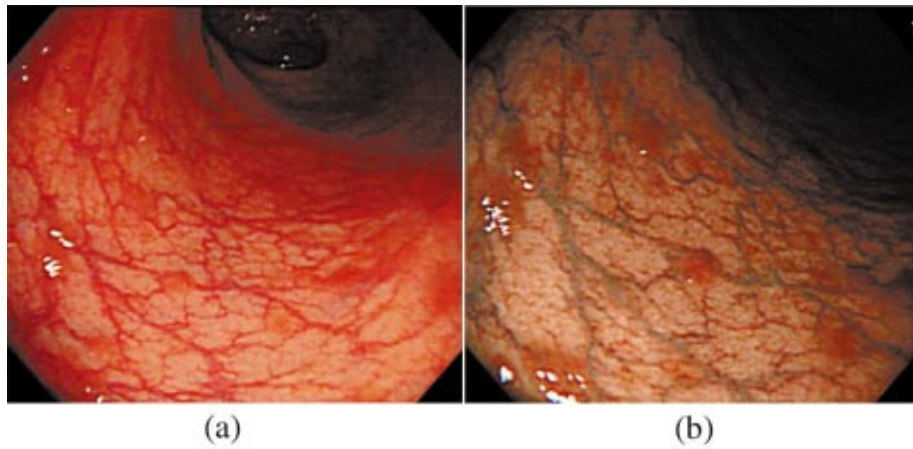


Fig. 6 (a) Conventional image and (b) NBI image of familial adenomatosis coli.

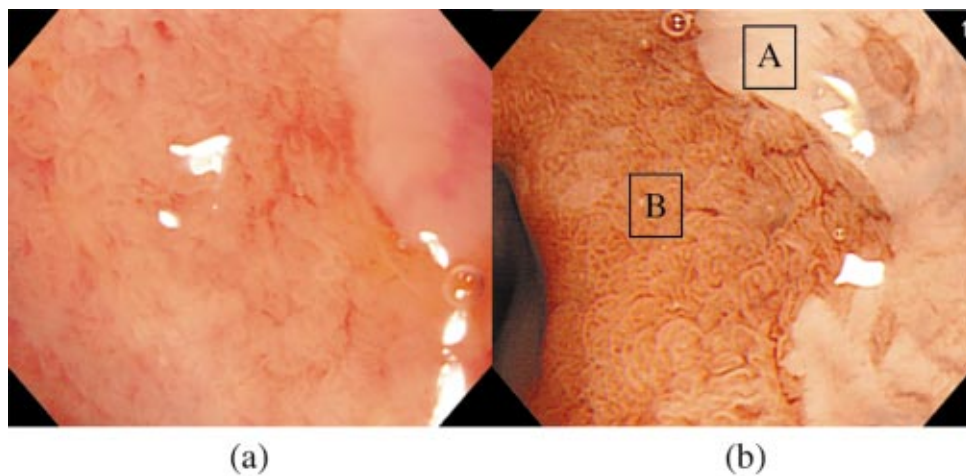


Fig. 7 (a) Conventional image and (b) NBI image of Barrett's esophagus.

Table 6 Scores of visualization of colonic small polyps.

	Unevaluated Score 1	Unclear Score 2	Clear Score 3	Total Score	Average Score	<i>p</i> value
Conventional	6	16	5	26	0.963	3.557×10^{-4}
NBI	2	7	18	43	1.593	

results indicated that NBI can more clearly define tumor margins than conventional illumination, and this difference is statistically significant ($p = 3.557 \times 10^{-4}$).

4.3.2 Barrett's esophageal endoscopy

As an example of a clinical test, Images obtained in a case of BE are shown in Fig. 7. The images are telescopic views obtained using the magnified function of the video endoscope. The region labeled "A" is the normal esophagus mucosa. The region marked "B" is the BE mucosa and shows a textured pattern. It is clear that NBI allows visualization of the pit pattern more clearly than conventional illumination. Table 7 shows the results of scoring by a gastroenterologist using a visual scale. The results agreed with comparative observations of images between conventional illumination and NBI. NBI showed a significant advantage in visualization of the pit pattern of the BE mucosa compared with conventional illumination ($p = 2.24 \times 10^{-4}$).

5 Discussion

In narrow-band images, the contrast of the C1 pattern shows a maximum at the maximum absorption wavelength of hemoglobin (415 nm). In addition, the contrast of the C1 pattern was blurred in the wavelength range outside that of hemoglobin absorption. On the other hand, the contrast of C2 and C3 patterns showed maxima in wavelength ranges different from the maximum absorption wavelength of hemoglobin. This is due to the differences in the position within the mucosa of the different classes of vascular pattern. The C1 pattern is in the superficial layer and therefore changes in its contrast with wavelength reflect the absorption spectrum of hemoglobin. On the other hand, C2 and C3 patterns are in the middle or deep layers of the mucosa, and therefore scattering and absorption by tissue and capillaries in the upper layer rather than in the middle or deep layers markedly affect the contrast. To allow visualization of the C2 or C3 pattern, the illumination has to penetrate the upper layer and reach the middle or deep layer. C2 and C3 patterns must have the thickness to compensate for the slight hemoglobin absorption. Therefore a vascular

pattern imaged in the longer wavelength range is thicker than the C1 pattern. Our assessments concerning the C3 pattern are in agreement with the results reported previously by Kienle et al.¹²

By comparing the contrasts of narrow-band (F1, F4, F5) and broadband (F6, F7, F8) images, we found that narrowing the bandwidth improved the contrast of the vascular pattern. This is due to cutting of the longer wavelengths. For example, F6 images have a lower contrast for the C1 pattern than F1 images. F6 images involve longer wavelengths than F1 images, and these longer wavelengths blur the contrast of the C1 pattern. The effects of narrowing the bandwidth on the contrast of the C2 pattern in F4 and F7 images and on the contrast of the C3 pattern in F5 and F8 images can be explained in the same way as for the C1 pattern. However, F7 and F8 band illuminations do not involve longer wavelengths, but involve shorter wavelengths than narrow-band illumination. At present, we cannot explain the mechanism responsible for this phenomenon.

Table 4 and the color images in Fig. 5 show that CIE 1976 $L^*a^*b^*$ color differences may not be suitable for evaluating the appearance of the vascular pattern in color images. On the other hand, the values of L^*ctr agree with observations of the C1 pattern. We examined the appearance of the vascular pattern from the viewpoint of the dependence of spatial frequency on the contrast sensitivity of human vision. Lakhan and Vimal²³ and Sakata and Isono²⁴ reported that the contrast sensitivity of human vision in the luminance channel is higher than that in the color channel within a range of from 5 to 10 cycles per degree (cpd). If we assume that the observational distance is 1.4 m from the monitor, the spatial frequency of a typical C1 pattern is in the range of 5 to 10 cpd. Referring to their results (Fig. 1 in Ref. 23 and Fig. 4 in Ref. 24), we found that the sensitivity in the luminance channel is tenfold greater than that in the color channel. The metric of L^*ctr has no color information. Therefore it is suggested that L^*ctr better reflects the observations of the C1 pattern than dE . In addition, C1 should be displayed as the luminance channel. To do this, we decided to use F1 and F2, and to assign both to the B

Table 7 Scores of visualization of Barrett's pit pattern.

	Completely Impossible Score 1	Visualization Just possible Score 2	Fairly Sharp Visualization Score 3	Complete Visualization Possible Score 4	Total Score	Average Score	<i>p</i> value
Conventional	0	4	17	0	55	2.620	2.246×10^{-4}
NBI	0	0	13	8	71	3.381	

and G channels. Moreover, we selected the F3 filter and assigned it to the R channel to display the C3 pattern as a bluish color. Of course other combinations of filter set and color assignment can be used by selecting the F1 filter. For example, gray-scale images can be made using only the F1 filter. However, endoscopists know from experience that information regarding the vein pattern is also important in detecting early colorectal cancer.²⁵ Therefore both the C1 and C3 patterns are important. Set A is the first trial case for clinical tests. Further studies on selection of the filter set and assignment to the color channel are required.

The tissue around the crypt orifice contains many capillaries. Therefore the pit pattern is thought to be the reverse of the capillary pattern within the tissue. F1 band images can be used to visualize the capillary pattern with high contrast and then can also be used to visualize the pit pattern. This was confirmed by a clinical test. Improvements in the appearance of the pit pattern in the BE mucosa are expected to enable detection of the SIM portion, which is associated with a high risk of developing cancer, by classifying the pit pattern. Chromoscopy also improves the contrast of the pit pattern by accumulating the dye in the crypt orifice, but if the mucosa is covered with mucus, it is difficult for the dye to accumulate. However, NBI is an optical enhancer of the contrast and is not affected by mucus. Moreover, NBI will reduce both the time and cost associated with standard chromoscopy.

The results of experiments 1 and 2 indicate that NBI with the magnified endoscope improves the contrast of the vascular pattern. On the other hand, the clinical test of small colonic polyps revealed that NBI is also useful in a wide view in which the capillary pattern cannot be recognized as individual thin vessels. The crowding of capillaries is visualized as a pattern with the appearance of brown staining. Adenomas and cancer tissue accumulate capillaries during their development. Therefore, small colonic polyps of adenomas or cancers can be seen as brown staining. Searches for small colonic polyps are usually performed under wide view. In addition, application of chromoscopy to the whole of the colon is not realistic. Therefore, NBI facilitates the finding of small colonic polyps, preventing them from being overlooked in patients with adenomas or cancers.

Hurzeler²⁶ used blue illumination to heighten the contrast of nodules, scars, and metaplasia in the bronchi. He used a blue filter with a broad bandwidth of about 250 nm. The results suggest that use of blue illumination will be useful for diagnosis in bronchoscopy. However, it is not clear whether his proposed illumination method can improve the contrast of the vascular or pit patterns; the broadband illumination used in the previous study may not be suitable for this purpose. Although the concept of the present study is similar to that of Hurzeler's study, the method proposed here can be used to quantitatively determine the contrast effect of using narrow-band illumination and has been shown to be of clinical benefit in gastrointestinal endoscopy.

6 Conclusions

Using five narrow-band illuminations and three broadband illuminations, we investigated the relationships between the spectral features of illumination and contrast for vascular patterns in endoscopic images. We classified the patterns into

three classes (C1, C2, and C3) and quantitatively evaluated the contrast of each class. By comparing the results for narrow-band images, we found that F1 (415 nm \pm 30 nm) is appropriate for imaging the C1 pattern; F3 (500 nm \pm 30 nm) or F4 (540 nm \pm 20 nm) is appropriate for imaging the C2 pattern; and F5 (600 nm \pm 20 nm) is appropriate for imaging the C3 pattern. In addition, we found that narrowing the bandwidth can improve the contrast of the vascular pattern. Evaluating three sets of filters for color imaging, we selected a set for clinical tests. Our selected set was 415 \pm 30 nm, 445 \pm 30 nm, and 500 \pm 30 nm. Clinical tests in colonoscopy indicated that NBI aided in finding small colonic polyps. Clinical tests in Barrett's esophageal endoscopy indicated that NBI facilitated classification of the pit pattern of the BE mucosa. These clinical benefits of NBI prevented small adenomas and cancers in the colon from being missed, enabling accurate biopsy for the portion at high risk of cancer development. We plan to conduct clinical tests in larger numbers of cases and in other diseases.

Acknowledgments

This work was supported in part by a grant from the Japanese health, labor, and welfare ministry for Scientific Research Expenses for Health and Welfare Programs, the Foundation for the Promotion of Cancer Research, and the Second-Term Comprehensive 10-year Strategy for Cancer Control.

References

1. S. Kudo, S. Hirota, T. Nakajima, S. Hosobe, H. Kusaka, T. Kobayashi, M. Himori, and A. Yagyu, "Colorectal tumors and pit pattern," *J. Clin. Pathol.* **47**(10), 880–885 (1994).
2. S. Kudo, S. Tamura, T. Nakajima, H. Yamano, H. Kusaka, and H. Watanabe, "Diagnosis of colorectal tumorous lesions by magnifying endoscopy," *Gastrointest. Endosc.* **44**(1), 8–14 (1996).
3. S. Kudo, H. Kashiba, T. Nakajima, S. Tamura, and K. Nakajo, "Endoscopic diagnosis and treatment of early colorectal cancer," *World J. Surg.* **21**(7), 694–701 (1997).
4. K. Tobita, "Study on minute surface structures of the depressed-type early gastric cancer with magnifying endoscopy," *Diges. Endosc.* **13**, 121–126 (2001).
5. N. Sakaki, "Magnifying observation and gastric mucosa, particularly in patients with atrophic gastritis," *Endoscopy* **10**(4), 269–274 (1978).
6. M. B. Fennerty, "Tissue staining (chromoscopy) of the gastrointestinal tract," *Can. J. Gastroenterol.* **13**(5), 423–429 (1999).
7. M. I. Canto, "Vital staining and Barrett's esophagus," *Gastrointest. Endosc.* **49**(3), 12–16 (1999).
8. Y. Kumagai, H. Inoue, K. Nagai, T. Kawano, and T. Iwai, "Magnifying endoscopy, stereoscopic microscopy, and the microvascular architecture of superficial esophageal carcinoma," *Endoscopy* **34**(5), 369–375 (2002).
9. K. Yagi, A. Nakamura, and A. Sekine, "Comparison between magnifying endoscopy and histological, culture and urease test findings from the gastric mucosa of the corpus," *Endoscopy* **34**(5), 376–381 (2002).
10. K. Gono, M. Yamaguchi, and N. Ohyama, "Improvement of image quality of the electroendoscope by narrowing spectral shapes of observation light," in *Proceedings of the International Congress of Imaging Science*, Imaging Society of Japan, pp. 399–400 (2002).
11. Y. Sano, M. Kobayashi, Y. Hamamoto, S. Kato, K. Fu, T. Yoshino, and S. Yoshida, "New diagnostic method based on color imaging using narrow band imaging (NBI) system for gastrointestinal tract," in *Proceedings Digestive Disease Week (DDW)*, Atlanta, GA, abstract: A696 (2001).
12. A. Kienle, L. Lilge, A. Vitkin, M. S. Patterson, B. C. Wilson, R. Hibst, and R. Steiner, "Why do veins appear blue? A new look at an old question," *Appl. Opt.* **35**(7), 1151–1160 (1996).
13. S. Prah, <http://omlc.ogi.edu/spectra/hemoglobin/summary.html>

14. M. A. Konerding, E. Fait, and A. Gaumann, "3D microvascular architecture of precancerous lesions and invasive carcinomas of the colon," *Br. J. Cancer* **84**(10), 1354 (2001).
15. A. Amar, A. F. Giovanini, M. P. Rosa, H. O. Yamasaki, M. B. Carvalho, and A. Rapoport, "Microvascular density in carcinoma of the tongue," *Rev. Assoc. Med. Bras.* **48**(3), 204 (2002).
16. A. K. Jain, *Fundamentals of Digital Image Processing*, Prentice-Hall, Englewood Cliffs, NJ (1988).
17. N. L. Johnson and F. C. Leone, *Statistics and Experimental Design in Engineering and the Physical Sciences*, Wiley, New York (1977).
18. *Colorimetry*, 2nd ed., Publication Commission Internationale de l'Eclairage (CIE) 15.2 (1986).
19. W. S. Atkin, B. C. Morson, and J. Cuzick, "Long-term risk of colorectal cancer after excision of rectosigmoid adenomas," *N. Engl. J. Med.* **326**(10), 658–662 (1992).
20. S. J. Winawer, A. G. Zauber, M. N. Ho, M. J. O'Brien, L. S. Gottlieb, S. S. Sternberg, J. D. Waye, M. Schapiro, J. H. Bond, and J. F. Panish, "Prevention of colorectal cancer by colonoscopic polypectomy," National Polyp Study Workgroup. *N. Engl. J. Med.* **329**(27), 1977–1981 (1993).
21. W. J. Blots, S. S. Devesa, R. W. Kneller, and J. F. Fraumeni, Jr., "Rising incidence of adenocarcinoma of the esophagus and gastric cardia," *J. Am. Med. Assoc.* **265**, 1287–1289 (1991).
22. T. Endo, T. Awakawa, H. Takahashi, Y. Arimura, F. Itoh, K. Yamashita, S. Sasaki, H. Yamamoto, X. Tang, and K. Imai, "Classification of Barrett's epithelium by magnifying endoscopy," *Gastrointest. Endosc.* **55**(6), 641–647 (2002).
23. R. Lakhan and P. Vimal, "Spatial frequency discrimination: a comparison of achromatic and chromatic conditions," *Vision Res.* **42**, 599–611 (2002).
24. H. Sakata and H. Isono, "Chromatic spatial frequency characteristics of human visual system (color difference discrimination)," *Television* **31**(1), 29–35 (1977) (in Japanese).
25. S. Kudo, *Early Colorectal Cancer*, p. 25, Igaku-Shoin, Tokyo (1996).
26. D. Hurlzeler, "Blue light endoscopy," *Laryngoscope* **85**(8), 1374–1378 (1975).